Local icosahedral structures in binary-alloy clusters from molecular-dynamics simulation

Stefano Cozzini
Dipartimento di Fisica, Università di Trento, 38100 Trento, Italy;
INFM, I-38050 Povo, Italy;
and Departamento de Fisica Atomica, Molecular y Nuclear, Universidad de Sevilla, Apartado 1065, 41080 Sevilla, Spain

Marco Ronchetti
Dipartimento di Informatica e Studi Aziendali, Università di Trento, 38100 Trento, Italy
(Received 22 November 1995, revised manuscript received 6 February 1996)

We investigate the structure of 13-particle clusters in binary alloys for various size ratios and different concentrations via molecular-dynamics simulation. Our goal is to predict which systems are likely to form local icosahedral structures when rapidly supercooled from the melt. We calculate the energy spectrum of the minimal energy structures, and characterize all detected minima from both their relative probability and a structural point of view. We identify regions in our parameter space where the icosahedral structure is dominant (like in the corresponding monatomic case), regions where the icosahedral structure disappears, and others where icosahedral structures are present but not dominant. Finally, we compare our results with simulations reported in the literature and performed on extended binary systems with various size ratios and at different concentrations. [S0163-1829(96)05018-7]

I. INTRODUCTION

Over the last decade, chemists and solid state physicists have been greatly interested in the platonic solid with the highest symmetry: The icosahedron. Chemists became interested in icosahedra because several clusters have been found to be icosahedral or polyicosahedral. In particular, the recent synthesis and structural determinations of metal carbonyl clusters resulted in a variety of icosahedral clusters containing transition metals and main group elements.[1] Solid state physicists believed until recently that icosahedral symmetry played no role in extended structures because it is not compatible with periodic arrangement of structural units (i.e., with crystalline order). It is now known that icosahedral symmetry is compatible with quasiperiodic translational order, and states of matter arranged in such a way have been found (i.e., quasicrystals[2]). Moreover, icosahedral structures are suggested to be important in disordered systems, like supercooled liquids and glasses.[3] The presence of icosahedra in simple supercooled liquid and glasses was revealed by means of computer simulations: From the pioneering work of Steinhard, Nelson, and Ronchetti[4] up to the most recent works,[5] there is evidence in the literature that it is so for monatomic supercooled liquids and glasses interacting via Lennard-Jones (LJ) and a variety of different metallic potentials.[6] So far, however, studies of LJ binary systems yield contrasting results.[7] The study of icosahedral clusters is therefore important both in itself and because it can give hints on the presence of such structures in disordered systems and on the nucleation of extended icosahedral quasicrystals. Computer simulations performed by Honeycutt and Andersen[8] on homogeneous LJ systems showed that icosahedrally symmetric clusters are the lowest in energy up to a size of 5000 atoms. A similar study in binary systems would be interesting, but unfortunately it is difficult because the parameter space to be investigated is far more complex. In fact in the case of monatomic species only the interaction potential and the cluster size (i.e., the number of particles) have to be specified, while in binary systems the relative abundance of the two species, geometric factors (i.e., size ratios), and parameters relative to the binding energy have to be taken into account. For this reason computational studies on mixtures are rare and focused on specific aspects, like the study of impurities in clusters[9] or the dynamics of phase separation.[10] To start exploring clusters in a binary system it is therefore necessary to reduce the search space by fixing a few parameters and studying the dependence on the remaining ones. For instance, both the above referred works by Garzon *et al.*[9] and Clarke *et al.*[10] keep the geometric parameters fixed and vary the energetics. In the present work we decided to cut the parameter space in an orthogonal direction by fixing the energetic parameters and the size of the cluster, and varying particle size and concentration. We therefore use the same depth of the potential well for both atomic species and for the interaction between unlike particles. For the cluster size we focus on 13-particle clusters, since our aim is to determine the importance of icosahedral structures. We therefore study the geometric structure and energy spectrum of 13-atom clusters for four different atomic size ratios and for all possible relative concentrations. In Sec. II we present the details of the computational model. In Sec. III we discuss the methods of measurements that we used. The results are presented in Sec. IV, followed by a discussion and a comparison with the literature (Sec. V).

II. COMPUTATIONAL MODEL

We studied a system composed of 13 particles belonging to two different species (L and S) and interacting with a LJ isotropic potential. The two species differ because of geometric factors: The radius of L atoms is larger than the radius of S atoms. The interaction between S atoms is characterized

by the parameters σ_{SS} and ϵ_{SS}: The interaction potential is therefore $V(r)=4\epsilon_{SS}[(\sigma_{SS}/r)^{12}-(\sigma_{SS}/r)^{6}]$. The potential for the atomic species L was defined by $\epsilon_{LL}=\epsilon_{SS}$ and $\sigma_{LL}=\alpha\sigma_{SS}$: The parameter α therefore fixes the ratio between the radii of the two species. The interaction between unlike particles was defined by $\epsilon_{LS}=\epsilon_{SS}=\epsilon_{LL}$ and $\sigma_{LS}=(\sigma_{LL}+\sigma_{SS})/2$. The values of σ_{SS} and ϵ_{SS} were suited to argon (this choice does not invalidate the generality of the results, since its only consequence is to fix the energy and length scales). The mass is not a relevant parameter when only structural properties are of interest, and we therefore used equal masses for the two species (again, we chose the argon mass). In the following all results are given in reduced units with ϵ_{SS} the unit of energy, σ_{SS} the unit of length and $(m\sigma_{SS}^2/48\epsilon_{SS})^{1/2}$ the unit of time.

The only relevant parameter is therefore α which fixes the size ratio between the two species. In the limiting case $\alpha=1$ the system is monatomic since the parameters for L and S atoms coincide. We used four different values for α: 1.6, 1.4, 1.33, and 1.25. A cluster in such model is further identified by the number N of particles composing it and by the relative concentration of L and S atoms. We fixed $N=13$ and studied all possible concentrations of $\eta\in\{1,12\}$, where η is the number of S atoms (the limiting cases $\eta=0$ and $\eta=13$ are equivalent, since they both correspond to a monatomic system). Our investigation covers therefore 48 points in parameter space. Our simulation method was the molecular-dynamics technique[11] in the microcanonical ensamble. We used the Verlet algorithm with a time step of 0.01 in our reduced units. Clusters were kept in free boundary conditions, and we checked that no atoms evaporated during the runs (cases in which atoms evaporated were discarded since we were interested only in 13 atom clusters). For each value of α and η we produced a large number of independent realizations using two different algorithms which yielded similar results. The first procedure consisted in starting (at equilibrium) from a liquid monatomic cluster composed of large particles. Then η large atoms were randomly substituted by small atoms, and the obtained cluster was allowed to relax for 10 000 time steps so as to equilibrate the new system. The cluster was then quenched into a minimum of its potential energy hypersurface. The whole process was repeated for a reasonably large number of times (typically 1000 times). We collected the final configurations and examined them by studying the resulting energy spectrum and the geometric configurations corresponding to the most relevant final states. The second procedure consisted in evolving for a very long time (typically 20×10^6 steps) a liquid cluster formed by η small particles and $13-\eta$ large particles, taking snapshots every 10 000 steps. The temperature is high enough that two configurations separated by 10 000 time-steps are statistically independent from each other. Each of the snapshots was then relaxed until the cluster reached the local minimum in potential energy, resulting in 1000 – 2000 independent configurations, which were then studied. Since we use a microcanonic molecular dynamics, by using the second procedure all the snapshots (for a given concentration) have the same total energy, while in the former case each initial configuration has different total energy. In spite of the different procedures, the two processes yield equivalent results: In particular the energies of the quenched clusters found with the two methods are the same, suggesting that the configurations we obtain do not depend on the particular history of the sample.

To reach the minimum energy configuration we used a steepest descent minimization: The kinetic energy was quickly stolen so that the cluster fell into the nearest potential energy well without having many chances to perform additional explorations in the configuration space while approaching a local energy minimum. The method corresponds roughly to a cooling rate of 10^{14} K/sec. For each of the 48 points in our parameter space we produced at least 2000 configurations. For a set of points a first analysis revealed complex behaviors: In such cases we collected more statistics, producing up to 4000 additional configurations. To avoid some very rare configurations gaining a considerable weight in our statistic, we consider only those minima which appear at least twice in our collection.

III. METHODS OF MEASUREMENTS

We were interested in identifying the structures which characterize the quenched clusters from both a structural and an energetic point of view. A first classification can be obtained by looking at the energy distribution of the collection of frozen samples: For each value of α and η we study the energy spectrum; i.e., we count the number of different potential energies reached at the end of the quenching process by our samples. There will be a lowest minimum, corresponding to the absolute minimum energy (i.e., the lowest minimum in the potential energy surface) and then set of many *excited* states. If there are significant gaps in the spectrum and moreover different structural properties are detected on either side of the gap, we can say that different *phases* are present in the system. Here we use the concept of *phase* discussed in depth by Honeycutt and Andersen:[8] A phase corresponds to a set of structures of minimum energy (inherent structures). Different phases are characterized by different sets of structures with different properties.

Not all energy minima will be reached with equal probability: We therefore associate to each minimum the corresponding frequency of visits, defined as the ratio between the number of times that a particular value of energy has been reached and the total number of samples produced. Having obtained this information, we can plot the frequencies versus energies: Such a plot reveals interesting features of the system under investigation.

We then study the geometric configuration of the quenched clusters. The structural analysis has been performed with various methods presented in the literature: Voronoi polyhedra, common neighbors analysis (CNA),[8] and Steinhardt's invariants.[4] These (and other) methods for investigating the presence of icosahedral structures were recently described in detail in a paper[7] where their validity was investigated. The technique of the Voronoi polyhedron is our main instrument. Given a cluster, our algorithm identifies the central atom(s) [as the atom(s) with the highest number of first neighbors] and then tries to determine the corresponding polyhedron (polyhedra). Polyhedra classification is based on the number of faces and on the number of edges of every face. A typical polyhedron is expressed with a set of 5 indexes indicating the number of faces with 3, 4, 5, 6, and 7

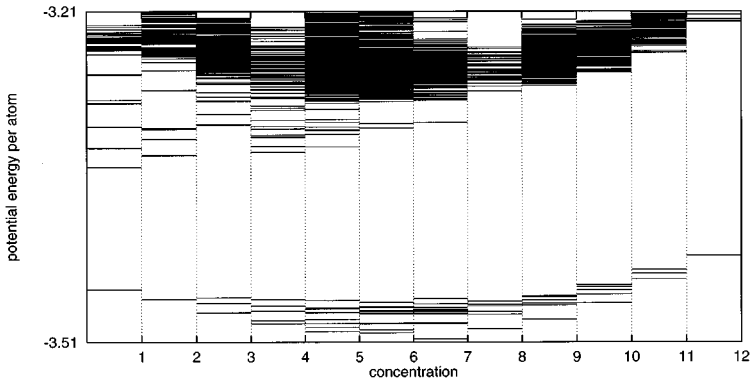

FIG. 1. The energy spectra for all the concentration at $\alpha=1.25$. All 12 different concentrations are plotted starting with $\eta=1$ (left) and ending with $\eta=12$ (right). The energy scale (the same for all the plots) is the absolute scale of energy and every straight line represents a different minimum. All the minima reported here are detected at least twice in our simulations.

edges. (The probability to find faces with more than 7 edges is negligible.) In this way we characterize the structure of every cluster: For instance the polyhedron for a particle at the center of a perfect icosahedral arrangement is the dual of the icosahedron, i.e., a dodecahedron (12 faces, each of them with 5 edges). The set is therefore (0,0,12,0,0). In a few pathological cases the program was not able to construct the polyhedron. The cause of the failures is essentially due to the fact that for some clusters the central atom has too few neighbors to allow our code to work (i.e., the cluster is very elongated).

As a second tool we used the CNA diagram in the formulation recently proposed by Faken and Jónsson.[12] We classify every cluster by looking at the CNA diagrams which involve the central atom. This technique allows us to discriminate between different configurations which exhibit the same Voronoi polyhedron (such cases are mostly due to different arrangements of particles on a second shell). This method also permits us to distinguish between configurations which are geometrically similar but differ for the relative placement of L and S atoms. Finally, we still needed to distinguish between clusters which were classified as icosahedral by the above methods, but which had a different degree of distortion. We found the use of the invariants proposed by Steinhardt *et al.*[4] very effective for such a measure. A number of clusters was also examined visually with the help of computer graphics programs.[12, 13] The number of configurations inspected in such way is obviously limited when compared to the great number of clusters produced: We looked mostly at the configurations identified as interesting by the previous analysis. We found the results of visual inspection very useful for reaching a better understanding of the phenomenology.

IV. RESULTS

We now present the results of our investigation. We divide the presentation in two steps: First we discuss the energetics of the clusters by studying the number of minima with respect to the energy (energy spectrum) and the number of visits at every minima (frequency of visits). Later we will examine the corresponding structures to understand in more detail the behavior of the systems.

A. Energetics

The energy of the clusters is first examined by looking at the energy spectrum as a function of η. Figure 1 shows some examples of the spectra: The spectra of all the concentrations for the case $\alpha=1.25$. For all the spectra we consider a window having a height of 0.3ϵ, which is large enough to give a complete representation of the energy distribution above the absolute minimum. The height of such window is comparable to that reported by Honeycutt and Andersen on the simulation performed on a monatomic 13-atom cluster.[8] In some cases this range includes the region where evaporation begins to occur. For each energy level E and for each concentration η we then study the frequency $\phi_\eta(E)$, defined as the number of times we find a configuration having an energy between E and $E+\delta E$ over the total number of configurations produced. Although δE is small (0.01ϵ), it gives a coarse-graining effect because of the even smaller energy differences among the minima. Frequencies $\phi_\eta(E)$ versus E are reported in Fig. 2 for all the concentrations of case $\alpha=1.6$. The highest peak at an energy E indicates that the most likely configuration (for the particular values α and η) has energy E. If only energetics was important, the most visited configuration should always be the one at the lowest energy. We will see that this is not always the case, showing that also entropy plays an important role in determining the most relevant state(s).

The most striking feature of the spectra is the existence of an energy gap which is most evident for $\alpha=1.25$: It is, however, smaller than for a monatomic system.[15] Below the gap the states are discrete, while above it a continuum of states exists, showing the signature of a liquidlike state. The continuum is not completely sampled by our simulations. At $\alpha=1.25$ (see Fig. 1) for high values of η all the states fall in the continuum, while for values of η smaller than 8 isolated states are present above the gap but below the continuum. The number of such isolated states grows as η decreases: They tend to populate the gap for small values of η. The behavior of the energy gap is shown in Fig. 3. The gap grows with η, and converges to a similar value for all concentrations when only one L particle is present ($\eta=12$). The convergence behavior is, however, quite different. Increasing α the gap tends to close for low η's due to two effects: The lowest energy moves toward higher energies and the number of discrete states below the continuum grows. At $\alpha=1.60$ such a trend is so pronunced that until $\eta=7$ there is no gap. The presence of a clear gap in a similar monatomic system is known to be the signature of the presence of icosahedra.[14] The value of the gap for monatomic systems is 0.219ϵ,[15] close to the value we get for $\eta=12$ for all α's. As we will

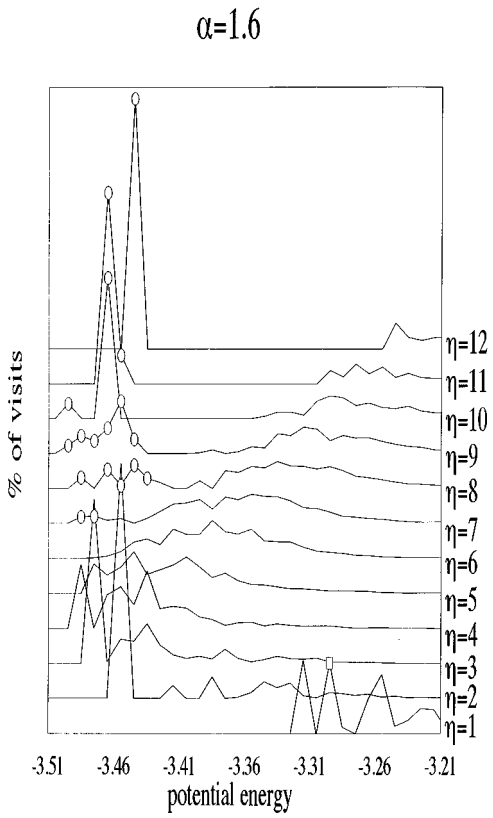

FIG. 2. The histograms of the percentage of visits to the minima for the case $\alpha=1.6$. For a better representation every different value of concentrations is shifted up by a number proportional to η: The lowest curve is therefore for the lowest concentration ($\eta=1$) while the upper curve is for $\eta=12$. Every peak of the curve is generally formed by more than a single minimum because of the relative large bin used in the histograms. All the peaks signed by an oval are due to icosahedral structures with a small atom at the center of the cage and the contribution to those peaks comes completely from icosahedral minima. On the curves we also indicated the positions of the icosahedral minima (squares) with a large atom at the center. In those cases, conversely, the contribution given by the icosahedral structures is not dominant at all.

see later, when discussing the icosahedral structures, this seems also to be the case for binary mixtures. This behavior is observed, with a few differences. Figure 4 shows the value of the lowest energy as a function of η for the various values of α. Of course the minimum energy has the same value for all α's when $\eta=0$ or $\eta=13$, since these cases describe the same system: A monatomic cluster. The energy always decreases when including an impurity of type L ($\eta=12$) and increases if the impurity is a small enough particle ($\eta=1$, $\alpha\leqslant 1.33$). The energy behavior is paraboliclike for $\alpha=1.25$, with a minimum for $\eta=7$. As α reaches the intermediate values ($\alpha=1.33$, $\alpha=1.4$) the shape does not change: The minimum remains at $\eta=7$ but the energy of the minima increases in a more pronounced way on the left side of the curve (i.e., in the region where the concentration of small atoms is smaller). At $\alpha=1.6$, however, the situation is quite different: The curve presents two different minima, respectively, at $\eta=4$ and $\eta=9$, implying the existence of two different mechanisms. Again, before discussing further this point, we will need to perform some structural examination.

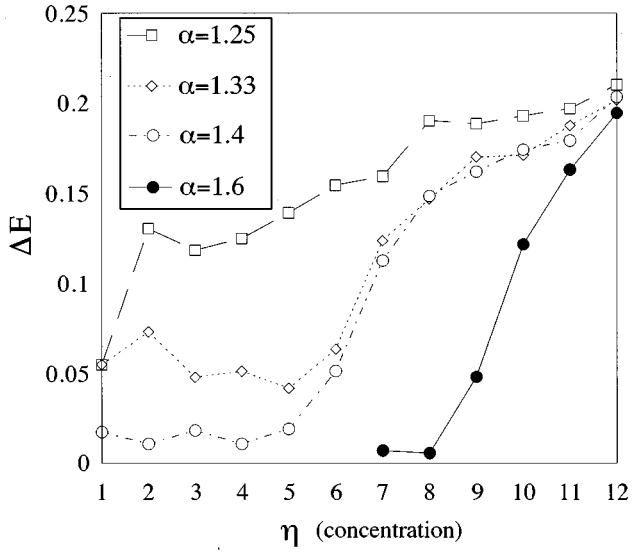

FIG. 3. The energy gap between the highest minimum in energy of the *S*-ICO structures and the first nonicosahedral cluster as a function of the concentrations. The four lines indicate the four different values of α. The 1.6 curve is not over all the range because there are icosahedral structures for $\eta<6$. Energy is given in LJ units.

The examination of frequency of visits enriches the above observations. For $\alpha=1.25$ we can see that the energy states below the gap are the most frequented. Above the gap instead the states in the continuum follow a rather flat distribution, except for $\eta=1$ and 2 where the lowest isolated states above the gap but below the continuum show a significant occupancy. Increasing α changes are noticed starting in the low-concentration range: States at the lowest energies (below the gap) are not the most visited ones: Rather, the most frequented states are the lowest in energy above the

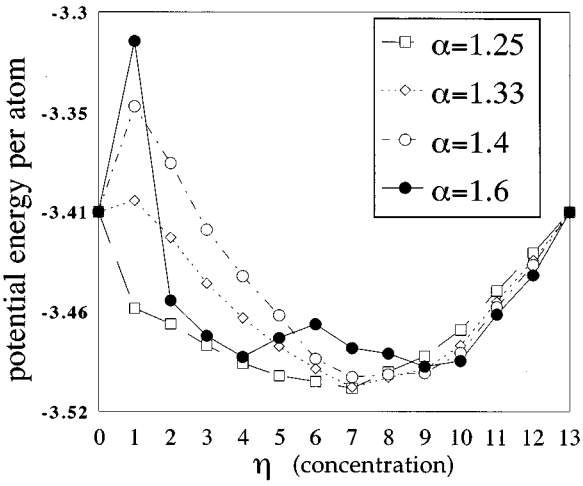

FIG. 4. The lowest minimum in the spectra plotted as a function of the concentration for the four values of α. The energy is in LJ units. The three lower values of α have a similar parabolic shape with the same minumum at $\eta=7$ and all the minima have an icosahedral cage, while the 1.6 case has a double-well shape and the icosahedral structures are limited only for $\eta>7$.

gap. The range of concentration over which this happens is increasing with α. The case $\alpha=1.6$ (reported in Fig. 2) shows an interesting behavior. At high values of η the scenario is similar to that of the other cases: The dominant peak is at the lowest energy. When η decreases the height of the dominant peak decreases and the gap shrinks. Above the gap a continuum of states has a rather flat distribution. The gap disappears for $\eta=8$. For $5\leqslant\eta\leqslant7$ no structure can be observed, as in the low range for $\alpha=1.33$ and 1.4. At $\eta=4$, however, a new feature appears: A peak develops at the lowest energy. The height of this peak grows when η decreases. No energy gap separates the high peak from the structures at higher energies. Finally, the case $\eta=1$ is singular: The most frequented states are the two at the lowest energies, where twin peaks are found. The energy of these states is much higher than for $\eta>1$.

B. Structural analysis

Having identified interesting regions and peaks, we analyze the samples to find which structures are responsible for the behavior we described above. Due to the very large number of minima found, it is obviously unfeasible to examine in detail all of the corresponding clusters. We therefore decided to focus our structural analysis on the configurations having a percentage of visits greater than 1.5%. In addition, we arbitrarily decided to examine also a few other configurations which we considered to be potentially interesting (like, for instance, the lowest-energy configurations also in cases where they are not frequently visited). Three-dimensional (3D) images of selected configurations helped to understand the structure of selected clusters.

A first indication comes from an analysis with Voronoi polyhedra. We calculate the percentage of the polyhedra with the same number of faces. We found that for $\alpha=1.33$ and high η's the percentage of 12-faced polyhedron is around 90%. At about midrange the presence of such a figure starts dropping, and steadily decreases down to a 10% for $\eta=2$. The growth of the signal of other-than-12-faced polyhedra at low concentrations is mainly due to 10-faced polyhedra: Only 11 atoms form the Voronoi cage while the two remaining particles are on the second shell. The scenario is similar for $\eta=1.4$, the difference being that the drop of the 12-faced polyhedron is much sharper, and very few such structures are found in the range $1\leqslant\eta\leqslant4$. Again, the competing structure is a 10-faced polyhedron which dominates the low-η region. The behavior is instead quite different in the two extreme cases: $\alpha=1.25$ and $\alpha=1.6$. In the first case the 12-faced polyhedron dominates over the whole range: Other structure comes close to a noticeability edge only for $\eta\leqslant2$. Quite the opposite situation is found at $\alpha=1.6$ (see Fig. 5): 12-faced polyhedra survive only for very high η's (i.e., for a cluster of S atoms with a few L impurities). At the other end of the range (i.e., in a cluster of L atoms with few S impurities) the dominating structure is the 9-faced polyhedron. The 3D graphical representation of such polyhedron for the case $\eta=2$ (Fig. 6) indicates that the lowest minima are achieved by clustering the small atoms in the center and accommodating all the large atoms in an external shell. Both 9-faced and 12-faced polyhedra are of little relevance in the middle of the region, where no structure is found to dominate: The peak of other structures is a mixture of unequal, elongated clusters. It is worth noting that for all values of α there a visible presence of 12-faced structures at $\eta=1$, even when the low-η range is characterized by structures other than 12-faced polyhedra.

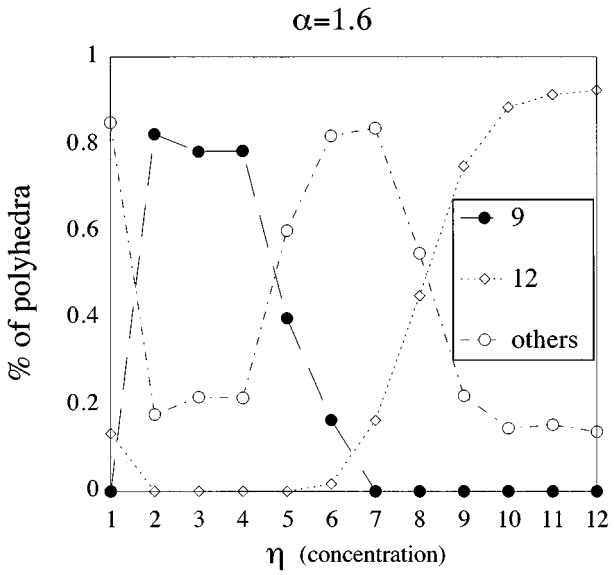

FIG. 5. Plot of the percentage of the clusters with a Voronoi polyhedra with 12 faces (indicated with 12), 9 faces (9), and the percentage of the remaining clusters (others) as a function of concentration for $\alpha=1.6$.

Of course the analysis with the Voronoi polyhedra does not tell the whole story. For instance, 12-faced polyhedra can be of different sorts: They can be icosahedra with an L particle at the center, icosahedra with an S atom at the center, or even irregular, nonicosahedral structures.

C. Icosahedral structures

There are two different classes of icosahedral clusters: The ones with a small particle in the center of the cage and

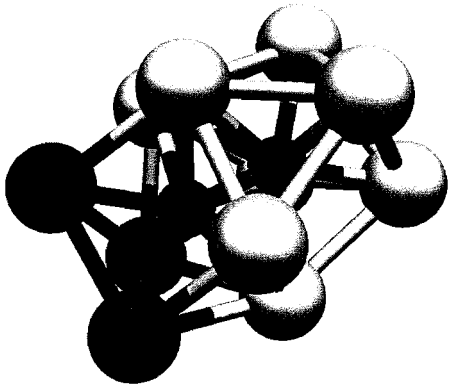

FIG. 6. The absolute minimum energy cluster for the case $\alpha=1.6$ and $\eta=2$. The two small particles are inside a cage formed by the large particles. The peculiarity of this structure is that each of the two small particles is at the center of a Voronoi cage of 9 faces. The particles belonging to such a structure are in the figure in light gray. The three particles on the second shell of such a cage are represented in dark gray.

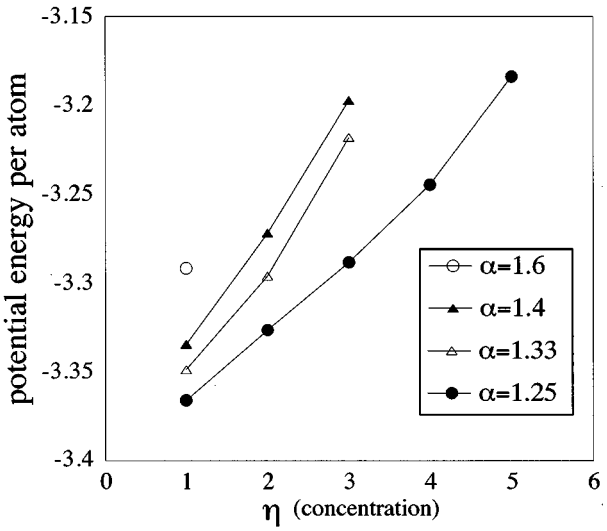

FIG. 7. The energy of the lowest L-ICO structures as a function of the concentration η. The four symbols are for the different values of α. The rapid increasing in energy as η grows limits the range of presence of such structures at very low concentrations.

those built around a large particle. We will call these structures S-ICO and L-ICO, respectively. We observed that whenever the energy gap is present, all states below the gap are S-ICO's. L-ICO's are present only for low η's, intermixed with nonicosahedral states: Their energy grows rapidly with η, so that they can never be found for $\eta>5$ in the energy range we considered. The presence and the importance of this kind of structure is therefore very marginal. Figure 7 summarizes this aspect: The lowest L-ICO configurations are plotted as function of the concentration.

It is also interesting to note that the number of different S-ICO configurations has a maximum for intermediate concentrations, and it decreases symmetrically when η gets larger or smaller. The number of different icosahedral configurations built around a small particle can be predicted. We can state the problem in the following way: In how many ways can the 13 vertices of an icosahedron be decorated with η S atoms and 13-η L atoms? If no vertices are equivalent the answer is trivial: The number of different decorations will be given by the binomial coefficient. But this is not the case of the regular icosahedral cage: In this case the problem is to calculate the number of different isomers (or different polytypes in mathematical terminology). As an example consider the case of $\eta=1$. In this case we have two different independent arrangements: As a first choice we can put the S particle in the center of the cage and the L particles on vertices of the icosahedron. The second possibility is to put an L particle in the center: For the S particle there are therefore 12 topologically equivalent vertices on the external cage. The resulting isomer is therefore 12 times degenerated. The number of different isomers has been recently calculated by Theo and co-workers[1] with an application of Polya's enumeration theorem. In Table I we report, as a function of η, the number of isomers and the number of different S-ICO's found for each value of α. For the lowest two values of α the number of S-ICO's coincides with the expected number of isomers: Peaks at different energies below the gap are due to different arrangements of L and S atoms on an icosahedral

TABLE I. Number of different isomers for an icosahedron having an particle S at the center, and $13-\eta$ atoms of the second kind (L) distributed on external vertices. The number of isomers is then compared with the number of different icosahedral minima (with an S particle at the center) detected for all the values of α.

η	Isomers	$\alpha=1.6$	$\alpha=1.4$	$\alpha=1.33$	$\alpha=1.25$
1	1	0	1	1	1
2	1	0	1	1	1
3	3	0	1	3	3
4	5	0	3	5	5
5	10	0	7	10	10
6	12	0	9	12	12
7	18	2	17	18	18
8	12	5	12	12	12
9	10	9	10	10	10
10	5	5	5	5	5
11	3	3	3	3	3
12	1	1	1	1	1

structure. For $\alpha=1.4$ the ratio between found S-ICO's and expected isomers drops for values of η smaller than 7, as shown in Fig. 8. An even more dramatic transition is shown for $\alpha=1.6$, where the ratio drops abruptly from 1 to 0 when η decreases from 9 to 6, showing the impossibility to build icosahedra for such radii ratio when the S particles are a minority.

Interesting observations can arise from the fact that for high values of concentration almost all the isomers are present. We checked to find correlations between the relative positions of L atoms (considered as impurities in a cluster formed by S atoms) and the energy or the distortion of the cluster. Our results do not allow a coherent interpretation of all data, but we were able to detect some regularities.[16] Let us first focus on $\eta>9$, where we find icosahedral isomers for all the values of α. For all these structures a general rule is

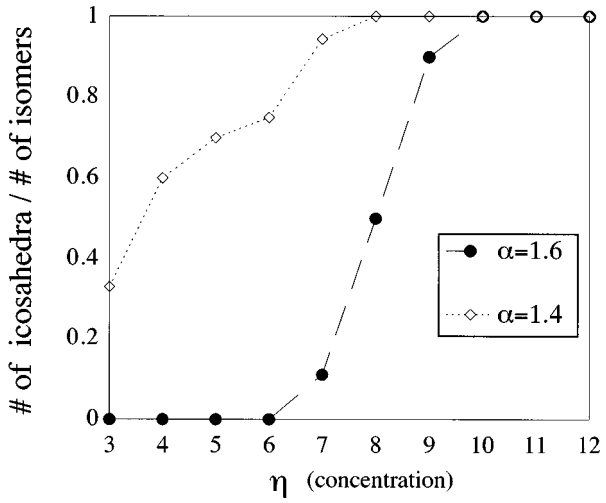

FIG. 8. The ratio between the number of different icosahedral minima detected for $\alpha=1.4$ and 1.6 and the number of isomers as a function of concentrations. All the icosahedral minima are of S-ICO type.

valid: The energy of the isomers is strictly correlated with the disposition of the impurities on the cluster. As a matter of fact in the lowest minima we find structures where the L impurities tend to occupy contiguous positions on the external shell, and the energy grows when the atoms are placed in nonadjacent positions. A very clear example is given in the case of two large atoms ($\eta=11$ and 3 different isomers): The lowest configuration is the configuration with impurities placed as first neighbors, the second with L atoms as second neighbors, and the highest one with L atoms as third neighbors. This situation is the same for all the values of α. Decreasing η this rule is violated: For $\eta=9$ it remains valid for $\alpha=1.33$ and $\alpha=1.25$ while for $\eta=8$ only the lowest value of α is consistent with this picture. Lowering η again no regularities are found. Along this line one can expect that the structures of the icosahedra have a high degree of distortion if the L atoms are close, while the distortion is small if they are placed in a symmetric way. All the observations of distortion (based on the measure of the third-order invariant) confirm this idea, and so we can say that the most distorted clusters correspond to the lowest minima. We have to stress that this picture is valid only as long as the L atoms can be considered as a perturbation on an icosahedron of S atoms, i.e., for large η's. A similar rule might be valid also for the case in which S atoms perturb an icosahedron of L atoms, but since L-ICO's are very expensive in energy, we do not have samples to verify this idea. With regard to the role of α, it is easy to guess that the distortion grows with α: Our results confirm this conjecture for all the values of concentrations.

D. Case $\alpha=1.6$ and $\eta=1$

As we anticipated the case $\alpha=1.6$ and $\eta=1$ is singular: It is therefore interesting to discuss this case in detail, with the help of 3D images. The lowest energy is much higher than that for $\eta>1$, and the frequency plot shows two twin peaks. However, these two peaks are degenerate, in the sense that each is formed by two different structures very close in energy. The four configurations occur with the same frequency. The clusters forming the lowest peak have the same basic structure, a cage formed by ten large atoms surrounds a small atom at the center, while the other two large atoms are on a second shell. The two different states are due to a different accommodation of these external atoms. The lowest minimum is presented in Fig. 9(a). The two clusters belonging to the second peak are completely different in that case: The configuration at higher energy is an icosahedron with a large particle [Fig. 9(b)] in the center while the lower one is formed by the small atom in the center surrounded by only eight atoms: Four atoms are on the second shell of the cluster. We observe that none of the four configurations is an S-ICO. The reason for its singularity lies in part on this simple observation. In all cases for $\alpha\leqslant 1.4$ the lowest-energy structures are S-ICO's. The same is true for $\alpha=1.6$ and $\eta\geqslant 6$. For $\alpha=1.6$ and $1\leqslant\eta\leqslant 5$ it is possible to construct structures with a droplet of two or three S atoms at the center (like in Fig. 6), allowing all the L atoms to be embedded in a first shell around the droplets. However, when the size ratio is so large and only one S-atom is available, putting the small atom at the center forces two large particles on a second shell: These particles have a small coordination and therefore the energy of the cluster is high.

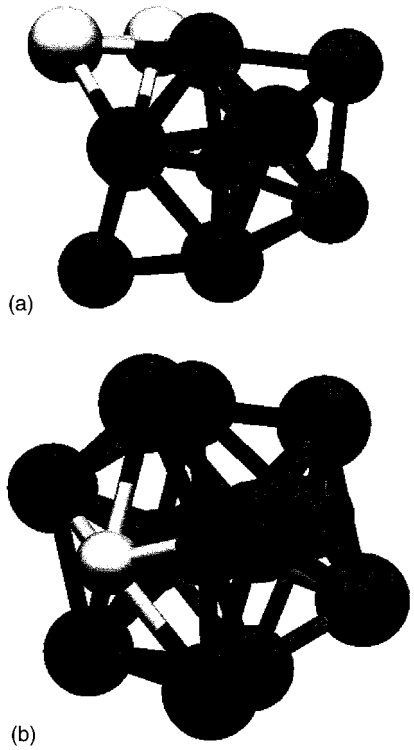

FIG. 9. Two different structures of the lowest minima for the case $\alpha=1.6$ and $\eta=1$. (a) is the lowest one, with Voronoi cage (0,2,8,0,0). (b) is a perfect icosahedron with a small particle on the external shell and with a large particle at the center.

V. DISCUSSION

A. Interpretation of the results

In a monatomic system, the best arrangement of 13 atoms is the icosahedron. Our work is aimed at understanding if and how this arrangement changes when a 13-atom cluster is composed of two different kinds of atoms. It is useful to remember that an optimal icosahedral configuration is achieved when the radius of the external particles is 1.06 times larger than the radius of the central particle: In an icosahedral cluster made of equal spheres, the spheres on the shell are therefore a bit loose. Let us first focus on the lower η values: The η small atoms can be seen as a perturbation of a cluster made of L particles. Such a perturbation can have opposite effects, depending on whether an S atom occupies the center of the cluster or not. We consider first the case $\eta=1$ in which the icosahedron has an L particle at the center, while on the vertices there are 11 L atoms and 1 S atom. In the monatomic cluster the particles on the shell are a bit loose: By shrinking the size of an external particle frustration and energy are increased. When η grows, so will frustration and energy. These considerations can explain what we observe: L-ICO clusters are found only for very small η's, and their energy grows rapidly with η. The role of the α parameter is also easy to understand: The larger the difference between the two component in the cluster, the faster the growth in energy. Let us now consider the case $\eta=1$ with

TABLE II. A collection of papers dealing with the problem of icosahedral order in binary systems. Column 1 gives the authors; column 2 specifies the interatomic potential used in simulations. The percentage of S particles used by the authors is given in column 3, and in column 4 as η, to facilitate the comparison with the present work. Column 5 indicates the value of the size ratio (α), and column 6 gives an indication about icosahedra detected in the samples.

Authors	Potential	Percent of S atoms	η	α	Icosahedra?
Jónsson and Andersen (Ref. 17)	LJ	80%	9.6	1.25	Yes
Shumway *et al.* (Ref. 5)	LJ	80%	9.6	1.25	Yes
Dasgupta *et al.* (Ref. 19)	LJ	50%	6.5	1.6	No
Ernst *et al.* (Ref. 20)	LJ	20%	2.6	1.25	suggested
Qi and Wang (Ref. 22)	Mg_3Ca_7	70%	3.9	1.33	Yes
Clarke and Wiley (Ref. 24)	hard spheres	various	various	1.1–1.5	negligible
Clarke and Jónsson (Ref. 23)	hard spheres	80%	9.6	1.25	Yes

the small atom as the central particle of the cluster. In such configuration the external particles are more squeezed than in the monatomic case. A value of α larger than 1 but smaller than 1.06 helps to remove the frustration typical of monatomic systems. For larger values of α frustration is induced by the fact that the small particle at the center is unable to ''fill'' the space in the cage created by the external particles. Our results show that for a value of α as large as 1.25 the energy decreases, which means that the overall frustration is diminished, while larger values of α induce a growth in energy. Increasing η, the new S atoms must substitute some L atoms on the external shell, which by shrinking decreases the frustration of the central atom: Energy therefore drops. S-ICO's are therefore favored in most cases, with a notable exception occurring when α is too large and η is small. In such a case, fewer than 12 particles are needed to surround the central atom: The remaining L atoms end up in a second shell, where their coordination is low and therefore the energy of the cluster grows. This case was discussed in detail in Sec. IV D. The transition from icosahedral structures to nonicosahedral ones is clearly shown from the shrinking energy gap between the S-ICO's and other nonicosahedral configurations with impurities at the center of the cage. The nonicosahedral minima are favored as the gap in energy becomes smaller and are dominant starting from $\alpha=1.33$.

Let us now consider the high η values. Similar but opposite considerations hold. At $\eta=12$ only one L atom is present: If it was at the center, frustration of the S atoms on the shell would increase. In fact, we never find L-ICO's in this range. The other case (the S atom as central particle) is the dominant one. The presence of L atoms on the shell increases the density and moves the cluster toward an energetically more convenient configuration. By decreasing η, this process continues: S-ICO's are stable in the whole high-η region.

In light of these considerations it is interesting to reconsider Fig. 3 and Fig. 4. As far as the three lowest values of α are concerned, Fig. 4 shows how the effect of impurities has a strong dependence on the choice of α in the case of small η's (i.e., a few impurities of type S), while when the impurities are of type L (large η's) the behavior does not strongly depend on α. The curve for $\alpha=1.6$ instead shows two different minima, indicating that at small η's icosahedra are again the dominant structure, while at large η's different kinds of structures play the dominant role. Figure 3 shows how the insertion of small particles changes the monatomic case: The first substitution of an S atom on the cluster lowers the gap between icosahedral and nonicosahedral clusters. This gap tends then to grow toward the monatomic value when more S atoms are inserted. The parameter α changes speed in reaching the limit of the monatomic case. In the case $\alpha=1.6$ this behavior is found only at high η's because of the absence of icosahedra elsewhere.

B. Comparison with extended systems

We focus now our attention on a set of papers treating the analysis of icosahedral order in extended binary systems. Our aim is to see what degree of agreement exists between the behavior we described and the presence or absence of icosahedral order detected in the extended system discussed in these works. In Table II we report a certain number of papers dealing with the problem of icosahedral order. From the data of the simulations of each of these works we have extrapolated our two parameters η and α. It is clear that the right comparison with the parameter α is possible only if the interactive potential is a LJ potential and if the mixed interaction is treated as in our work. Anyway for the sake of completeness we reported in the table also studies performed on different systems: In this case the definition of the α has to be done carefully.

Let us first discuss the system which is strictly comparable with our results: LJ systems. We first concentrate on the work of Jónsson and Andersen[17] and of Shumway *et al.*,[5] in which both groups reported a considerable amount of icosahedral order in their samples. The parameters of two simulations are equal and correspond to $\alpha=1.25$ and $\eta=9.6$. Thanks to the courtesy of Hannes Jónsson who provided us some configurations we have analyzed carefully some samples from both these works in order to see in more detail what kind of icosahedra are present: We detected in all the samples only S-ICO types of icosahedra. The characteristics of the icosahedra (structures and concentrations) are in perfect agreement with the results discussed previously.[18] Our results are also in excellent agreement with the work by Dasgupta *et al.*[19] In their paper they reported the absence of long-range icosahedral correlation, which in the light of our study is no surprise, since at the values of concentration and radii chosen by them ($\alpha=1.6$, $\eta=6.5$) there can hardly be an

icosahedron. Their result should therefore not be taken as a general indication of the absence of icosahedral order in LJ systems.

Finally a comparison between our results and the ones by Ernst *et al.*[20] gives some interesting results. Let us discuss what kind of icosahedra should be expected to be found in an extended system like the one simulated by the authors in light of our results. In the region defined by their parameters (α=1.25, η=2.6) we found an icosahedral cluster with both *S*-ICO and *L*-ICO clusters, with a strong predominance of the former, due to energetic reasons. When we cool down such an extended system we would not expect local minima of type *L*-ICO (due to their high cost in energy). We would instead expect to find a certain number of *S*-ICO configurations, since these are energetically favored: However, this number could not be very high, because of the small concentration of *S* atoms which are needed as seeds of such a kind of icosahedra. This picture fits very well with the results of the work performed by Ernst *et al.* They in fact say that ''. . . the data for Q_l suggest icosahedral symmetry . . . and the average in Q_l is less for a pure icosahedron.'' A similar result is also obtained by Jónnson[21] on an equivalent system (same values of α and η), in which again only relatively few icosahedral shells are found, and all of them have *S* atoms at the center.

Let us now discuss some works with different potentials. One of the most interesting papers we found is the one of Qi and Wang[22] in which the authors simulated a Mg_3Ca_7 system, finding strong evidence of icosahedral order. They reported a complete cluster analysis identified by means of CNA. Having checked that their definition of the polyhedra is equivalent to our Voronoi construction we then can compare our polyhedra with theirs. The main problem in this case is to define the parameter α, since the authors did not report the core radius of the pair potential used. We estimate α to be equal to 1.33 where Ca is the *L* atom and Mg the small one. (This value of the ratio is the same suggested by Nelson and Spaepen[3] for the same system modeled by a hard sphere. It is also very close to the ratio of the atomic radii of the two elements.) Also in this case let us imagine what kind of structures would be expected in such systems based on our findings: With α=1.33 and η=4 we are in a zone with dominant *S*-ICO clusters but with a few other minima of some importance in the gap. So what we expect to see is some icosahedral structures (all with small atoms at the center) and some other significant minima. This picture agrees with the results by Qi and Wang partially: the most frequented clusters are coordinate 12, and the structures are icosahedral and (0,2,8,2,0) polyhedra. A rough estimation of the frequency of these polyhedra is qualitatively similar with our frequency of visits. A great majority of the icosahedral cluster has a small atom (Mg) at the center. The surprise, however, is the existence of some *L*-ICO structures. The relative absence of low-coordination polyhedra is probably due to the difference between an extended system and an isolated cluster. However, all the low-coordination polyhedra they detected are present in our configurations.

Finally we compare our result with two works performed on hard sphere systems. In this case the natural choice of the parameter α is given by the ratio of the radii of the two different spheres. Our results fit well with the result of Clarke and Jónnson[23] in which they found icosahedral order in a binary system of hard spheres with parameters α=1.25 and η=9.6. In the work of Clark and Wiley[24] in which they explore several concentrations and α values the results are more difficult to compare directly because the authors do not present extended results for all the points explored and they limit themselves to general considerations, concluding that icosahedral order is negligible in all their systems. However, extrapolating the data from the figures presented we can detect a qualitative agreement also in this case.

As a final remark we can say that our results show a substantial agreement with all the results presented in the literature and can therefore be used as a good indication for predicting the existence of icosahedra (and maybe of icosahedral order) for given size ratios and concentrations in binary systems.

VI. CONCLUSION

We studied 13-atom clusters of binary mixtures at four radii ratios α and for all possible concentrations η of small particles. We found that icosahedral structures are important for small α and become less relevant when α grows: For large values of α icosahedral structures play a role only when η is large. A general interpretation of this behavior is given in terms of impurities on the clusters. Finally our results can be successfully compared with the claims of the presence or absence of icosahedra in quenched extended binary systems, therefore allowing a better uderstanding of the contrasting results which appear in the literature.

ACKNOWLEDGMENTS

One of us (S.C.) spent part of the time during this work at the Department of Chemistry of the University of Washington. We are grateful to Hannes Jónsson for hospitality and for having provided the samples to analyze and for many useful discussions. This work has been supported in part by the Italian CNR Progetto Finalizzato Sistemi Informatici e Calcolo Parallelo (U.O. Reatto).

[1] B. K. Theo, H. Zhang, Y. Kean, H. Dang, and X. Shi, J. Chem. Phys. **99**, 2929 (1993). See also Refs. 4–8 therein.

[2] M. V. Jaric, *Aperiodicity And Order* (Academic, Boston, 1989), Vols. 1–3.

[3] D. R. Nelson and F. Spaepen, *Solid State Physics—Advances In Research And Applications*, edited by H. Ehrenreich and D. Turnbull (Academic, Boston, 1989), Vol. 42, p. 1.

[4] P.J. Steinhardt, D.R. Nelson, and M. Ronchetti, Phys. Rev. Lett. **47**, 1297 (1981); Phys. Rev. B **28**, 784 (1983).

[5] S. L. Shumway, A. S. Clarke, and H. Jónsson, J. Chem. Phys. **102**, 1796 (1995).

[6] For a short review see Ref. 3 and references therein.

[7] For a review of the methods to analyze local and extended structures, see M. Ronchetti and S. Cozzini, in *Defects and Disorder*

In Crystalline and Amorphous Solids, edited by C. R. A. Catlow, (Kluwer Academic, Dordrecht, 1994), p. 391.
[8] J. D. Honeycutt and H. C. Andersen, J. Phys. Chem. **91**, 4950 (1987).
[9] I. L. Garzon, X. P. Long, R. Kawai, and J. H. Weare, Z. Phys. D **12**, 81 (1989).
[10] A. S. Clarke, R. Kapral, G. N. Patey, B. Moore, and X.G. Wu, Phys. Rev. Lett. **70**, 3283 (1993).
[11] For an overview of the method see M. Ronchetti and G. Jacucci, *Simulation Approach To Solids. Molecular Dynamics Of Equilibrium Solids and More* (Jaca Book-Kluwer, Dordrecht, 1990).
[12] D. Faken and H. Jónsson, Comput. Mater. Sci. **2**, 279 (1994).
[13] V. Cavecchia (unpublished).
[14] M. R. Hoare, Adv. Chem. Phys. **40**, 49 (1979).
[15] I. L. Garzon, M. Avalos-Borja, and E. Blaisten-Borojas, Z. Phys. D **12**, 181 (1989).
[16] S. Cozzini, Ph.D. thesis, Università di Padova, 1995.
[17] H. Jónsson and H. C. Andersen, Phys. Rev. Lett. **60**, 2295 (1995).
[18] S. Cozzini and H. Jónsson (unpublished).
[19] C. Dasgupta, A. V. Indrani, S. Ramaswamy, and M. K. Phani, Europhys. Lett. **15**, 207 (1991); **15**, 467 (1991).
[20] R. M. Ernst, S. R. Nagel, and G. S. Grest, Phys. Rev. B **43**, 8070 (1991).
[21] H. Jónsson (private communication).
[22] D. W. Qi and S. Wang, Phys. Rev. B **44**, 884 (1991).
[23] A. S. Clarke and H. Jónsson, Phys. Rev. E **47**, 3975 (1993).
[24] A. S. Clarke and J. D. Wiley, Phys. Rev. B **38**, 3659 (1988).